Interaction of Calicheamicin with Duplex DNA: Role of the Oligosaccharide Domain and Identification of Multiple Binding Modes

Luigi Gomez Paloma,[⊥] Jarrod A. Smith,[‡] Walter J. Chazin,*[,‡] and K. C. Nicolaou*[,†,§]

Contribution from the Departments of Chemistry and Molecular Biology, The Scripps Research Institute, 10666 North Torrey Pines Road, La Jolla, California 92037, and Department of Chemistry, University of California at San Diego, La Jolla, California 92093

Received January 3, 1994[⊗]

Abstract: A 1:1 complex between calicheamicin θ_1^I (**1**) (an *S*-acetyl derivative of calicheamicin γ_1^I, **2**) and the duplex d(GCATCCTAGC)·d(GCTAGGATGC) has been studied by 1D and 2D ^{1}H NMR spectroscopy to establish the molecular basis for binding and the sequence selectivity of the interaction between this potent antitumor antibiotic and DNA. Complete sequence-specific assignments have been obtained for all drug and DNA protons (except 5′H and 5″H DNA protons). A complex between the same duplex and the calicheamicin γ_1^I oligosaccharide moiety (**3**) has also been examined in detail by ^{1}H NMR spectroscopy, and the results are virtually identical. Comparative analysis of the complex formed with and without aglycone demonstrates the critical role of the oligosaccharide domain in the molecular interactions leading to binding and sequence-specific recognition in the minor groove of the DNA duplex. A structural model for the complex was generated by refining manually docked initial structures using molecular dynamics calculations with NMR-derived distance restraints. A total of 194 DNA–DNA distance constraints (including 16 H-bond constraints), 13 drug–drug intra- and interresidue distance constraints, and 15 drug–DNA distance constraints were included in the calculations. Structures refined starting from standard A-form and B-form DNA geometries converged to a root mean square deviation of 1.12 Å for the well-defined regions of the complex. The current structural model is stabilized by several specific interactions including H-bonds and favorable van der Waals interactions. Temperature-dependence studies of the ^{1}H NMR spectrum revealed that calicheamicin θ_1^I (**1**) binds in two different modes within the d(TCCT)·d(AGGA) recognition site; two unequally populated species in slow exchange on the NMR time scale are observed at low temperature. The lifetimes of the major and minor binding modes were determined to be <19 and <6 ms, respectively, at 320 K, with an activation energy ($\Delta G^{\ddagger}$) of *ca.* 15 kcal/mol. We propose that this phenomenon is due to a movement of the aglycone portion of the drug in the DNA minor groove. This dynamic process thus provides a critical new insight to explain the observed DNA cleavage properties of calicheamicin.

Introduction

The enediyne family is a new and important class of antitumor antibiotics that cleave DNA and cause cell death. This family includes calicheamicins, esperamicins, dynemicin A, neocarzinostatin chromophore, and kedarcidin chromophore as well as a number of synthetic derivatives possessing highly potent antitumor activity.[1,2] It was determined that calicheamicin γ_1^I (**2**) binds to the minor groove of DNA duplexes at oligopyrimidine/oligopurine runs, including d(TCCT), d(TTTT), d(CTCT), and d(ACCT),[3] by orienting its oligosaccharide tail toward the 3′-end of DNA fragments.[4] A remarkable sequence selectivity is observed in the DNA cleaving patterns obtained with this molecule. Once bound, calicheamicin cleaves DNA in a double-stranded fashion by abstracting hydrogen atoms from both strands of the helix.[4,5] This DNA cleaving property is derived from the generation of sp^2 carbon-centered radicals upon bioreductive activation through a Bergman cyclization[6] (Scheme 1). The oligosaccharide fragment is thought to control the molecule's recognition and binding properties.[7,8] Speculation regarding the role of the iodine atom

Scheme 1. Mechanism of DNA Cleaving Action of Calicheamicins θ_1^I (**1**) and γ_1^I (**2**)

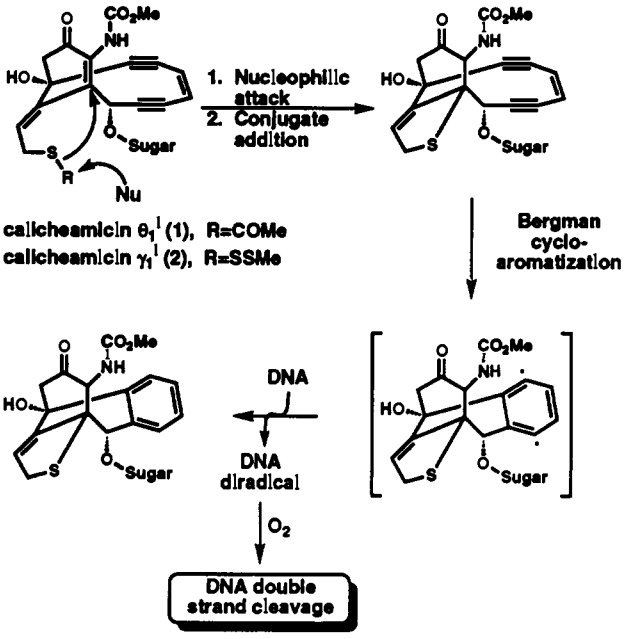

† Department of Chemistry, The Scripps Research Institute.
‡ Department of Molecular Biology, The Scripps Research Institute.
§ Department of Chemistry, University of California at San Diego.
⊥ On leave from the University of Naples, Italy.
⊗ Abstract published in *Advance ACS Abstracts,* March 15, 1994.

(1) (a) Nicolaou, K. C.; Dai, W. M. *Angew. Chem., Int. Ed. Engl.* **1991**, *30*, 1387. (b) Nicolaou, K. C.; Smith, A. L.; Yue, E. W. *Proc. Natl. Acad. Sci. U.S.A.* **1993**, *90*, 5881.
(2) Lee, M. D.; Ellestad, G. A.; Borders, D. B. *Acc. Chem. Res.* **1991**, *24*, 235.
(3) (a) Zein, N.; Sinha, A. M.; McGabren, W. J.; Ellestad, G. A. *Science* **1988**, *240*, 1198. (b) Walker, S.; Landovitz, R.; Ding, W. D.; Ellestad, G. A.; Kahne, D. *Proc. Natl. Acad. Sci. U.S.A.* **1992**, *89*, 4608.
(4) De Voss, J. J.; Townsend, C. A.; Ding, W. D.; Morton, G. O.; Ellestad, G. A.; Zein, N.; Tabor, A. B.; Schreiber, S. L. *J. Am. Chem. Soc.* **1990**, *112*, 9669.
(5) Hangeland, J. J.; De Voss, J. J.; Health, J. A.; Townsend, C. A.; Ding, W. D.; Ashcroft, J. S.; Ellestad, G. A. *J. Am. Chem. Soc.* **1992**, *114*, 9200.

0002-7863/94/1516-3697$04.50/0

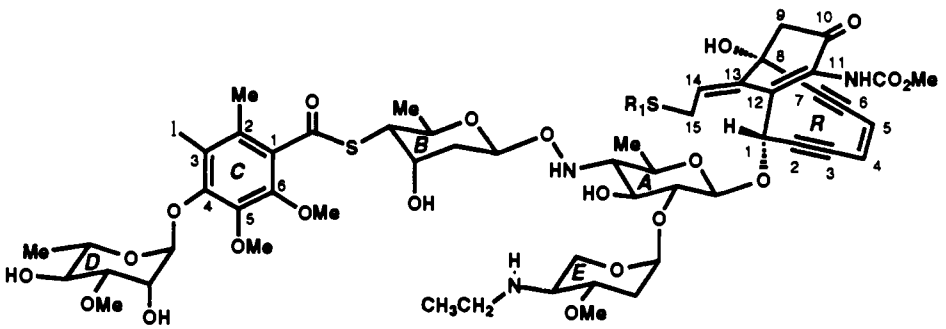

1: calicheamicin θ_1^1, R_1=$COCH_3$

2: calicheamicin γ_1^1, R_1=$SSCH_3$

Figure 1. Structures of calicheamicins θ_1^I (**1**) and γ_1^1 (**2**).

of the aromatic ring in the binding to DNA has raised intriguing questions. Schreiber and co-workers proposed an interaction between this iodine and the NH_2 group of the guanine(s) of the oligopurine strand.[9] Our footprinting and kinetic experiments have demonstrated that the iodine is an important structural element in the formation of the DNA–calicheamicin complex.[8,10]

NMR spectroscopy in solution is an important method for the characterization of DNA and complexes with ligands in solution,[11] having been developed to the point where three-dimensional structures in solution have been determined for both intercalators (e.g., chromomycin,[12] mithramycin,[13] [*N*-MeCys^3,*N*-MeCys^7]-TANDEM[14]) and minor groove binding agents (*e.g.*, distamicin A,[15] netropsin,[16] Hoechst 33258[17]). However, structural analyses of calicheamicin–DNA complexes have been largely restricted to molecular modeling, with only a single NMR study published[18] and no reports of X-ray crystal structures. In their NMR study, Kahne and co-workers identified a number of intermolecular contacts and proposed that the sequence specificity of calicheamicin γ_1^1 is due to the unique conformational flexibility of oligopyrimidine tracts which allows sufficient structural distortion to accommodate the rather rigid drug molecule.[18] However, with no refined structures available, there remain many open questions concerning the binding to duplex DNA and the relationship to the DNA cleaving activity of calicheamicin. In order to gain further insight into these questions, we prepared and analyzed by NMR methods two ligand–DNA complexes, one between the duplex d(GCATCCTAGC)·d(GCTAGGATGC) and calicheamicin θ_1^1 (**1**)[19] and the other between the same duplex and the methyl glycoside of the calicheamicin oligosaccharide (**3**).[20] After complete sequence-specific ^{1}H NMR assignments were obtained for both complexes, a structural model for the calicheamicin θ_1^1 complex was generated by refining manually docked initial structures using molecular dynamics calculations with NMR-derived distance restraints. The results for the two complexes are discussed in terms of their implications regarding the determinants of molecular recognition of duplex DNA and the observed DNA cleavage properties of calicheamicin.

The selection of the calicheamicin θ_1^I (**1**) synthetic analog for these studies, as opposed to the natural calicheamicin γ_1^1 (**2**), was made on the basis of the greater chemical stability of **1** under the conditions of the NMR experiments. The difference between the structures of **1** and **2** involves only the trisulfide trigger located on one of the side chains of the aglycone (Figure 1). This functional group plays a critical role in initiating the reaction cascade leading to the DNA damage (Scheme 1) but has no influence on the binding properties of the calicheamicins. Thorough analysis of 1D and 2D NMR spectra of the complexes of **1** and **2** with the same d(GCATCCTAGC)·d(GCTAGGATGC) duplex revealed that their spectral parameters are virtually identical. The results and conclusions made with calicheamicin θ_1^1 (**1**) are, therefore, fully applicable to calicheamicin γ_1^1 (**2**).

Experimental Section

Preparation of the Complexes. Calicheamicin θ_1^I (**1**) and the aglycone-free oligosaccharide were synthesized as described elsewhere.[19,20] The purified oligonucleotides d(GCATCCTAGC) and d(GCTAGGATGC) were purchased from Operon Technologies, Inc. (Alameda, CA) and were used without further purification. The two complementary strands were mixed in water in equimolar amounts and annealed by heating at 90 °C for 5 min and then allowed to cool to room temperature. The NMR sample was prepared by lyophilizing the duplex two times from 99.6% D_2O and then dissolving the lyophilized material in 500 μL of 10 mM phosphate buffer containing 100 mM NaCl and 0.1 mM EDTA at pH 7.0 in 99.996% D_2O. For experiments to assign the labile protons, the sample was lyophilized and redissolved in 90% H_2O/10% D_2O. The final concentration of the duplex was 2.0 mM.

The drug–DNA complexes were prepared according to the following procedure. Known amounts of ligand dissolved in MeOH were added to 1 mL of a 1.0 mM solution of the duplex, stirred at 25 °C for 5 min and then lyophilized and dissolved in 99.6% D_2O. The extent of the titration was monitored by examining the DNA 6H/8H resonances in the ^{1}H NMR spectrum. The final solution was lyophilized and redissolved in 500 μL of 99.996% D_2O. For the experiments to examine the labile DNA protons of the complex, the solution was lyophilized and redissolved in 500 μL of a 90% H_2O/10% D_2O solution.

NMR Experiments. All NMR experiments were performed on a Bruker AMX-500 spectrometer. The temperature was 293 K for all experiments on the free DNA duplex and 283, 293, 300, or 318 K for the experiments on drug–DNA complexes. All spectra were acquired in the phase-sensitive mode. The transmitter was placed on the solvent resonance, and the TPPI method was used to achieve frequency discrimination in the ω_1

(6) Bergman, R. G. *Acc. Chem. Res.* **1973**, *6*, 25.
(7) Drak, J.; Iwasawa, N.; Danishefsky, S.; Crothers, D. M. *Proc. Natl. Acad. Sci. U.S.A.* **1991**, *88*, 7464.
(8) Nicolaou, K. C.; Tsai, C. S.; Suzuki, T.; Joyce, G. F. *J. Am. Chem. Soc.* **1992**, *114*, 7555.
(9) Hawley, R. C.; Kiessling, L. L.; Schreiber, S. L. *Proc. Natl. Acad. Sci. U.S.A.* **1989**, *86*, 1105.
(10) Li, T.; Zeng, Z.; Estevez, V. A.; Baldenius, K. U.; Nicolaou, K. C.; Joyce, G. F. *J. Am. Chem. Soc.*, following paper in this issue.
(11) Gilbert, D. E.; Feigon, J. *Curr. Opin. Struct. Biol.* **1991**, *1*, 439.
(12) Gao, X.; Mirau, P.; Patel, D. J. *J. Mol. Biol.* **1992**, *223*, 259.
(13) Sastry, M.; Patel, D. J. *Biochemistry* **1993**, *32*, 6588.
(14) Addess, K. J.; Sinsheimer, J. S.; Feigon, J. *Biochemistry* **1993**, *32*, 2498.
(15) Dwyer, T. J.; Geierstanger, B. H.; Bathini, Y.; Lown, J. W.; Wemmer, D. E. *J. Am. Chem. Soc.* **1992**, *114*, 5911.
(16) Mrksich, M.; Wade, W. S.; Dwyer, T. J.; Geierstanger, B. H.; Wemmer, D. E.; Dervan, P. E. *Proc. Natl. Acad. Sci. U.S.A.* **1992**, *89*, 7586.
(17) Fede, A.; Billeter, M.; Leupin, W.; Wüthrich, K. *Structure* **1993**, *1*, 177.
(18) Walker, S.; Murnick, J.; Kahne, D. *J. Am. Chem. Soc.* **1993**, *115*, 7954.
(19) Nicolaou, K. C.; Li, T.; Nakada, M.; Hummel, C. W.; Hiatt, A.; Wrasidlo, W. *Angew. Chem., Int. Ed. Engl.*, in press.
(20) Gronemberg, R. D.; Mayazaki, T.; Stylianides, N. A.; Schultz, T. J.; Stahl, W.; Schreiner, E. P.; Suzuki, T.; Iwabuchi, Y.; Smith, A. L.; Nicolaou, K. C. *J. Am. Chem. Soc.* **1993**, *115*, 7593.

dimension.[21] The standard pulse sequence and phase cycling were used for 2Q,[22] 2QF-COSY,[23] and NOESY[24] spectra. A total of 32 or 64 scans/t_1 value were acquired for the 2Q (t_{mix} = 30 ms, t_{1max} = 50 ms) and 2QF-COSY (t_{1max} = 80 ms) spectra. TOCSY spectra were acquired using the DIPSI-2 sequence[25] for spin locking with t_{mix} = 70 or 120 ms, 32 scans/t_1 value, and t_{1max} = 50 ms. NOESY spectra from H_2O solutions were recorded with the last pulse replaced by a jump and return composite sequence.[26] NOESY spectra from D_2O solution were recorded with saturation of the residual HOD resonance during the preparation and mixing periods. NOESY spectra were acquired with mixing times of 50–300 ms, 32–108 scans/t_1 value, and t_{1max} = 50 ms. A NOESY spectrum was also acquired with t_{mix} = 800 ms to analyze the chemical exchange phenomenon. ROESY[27] spectra were acquired using a 100-ms low-power CW pulse for spin locking, 64 scans/t_1 value, and t_{1max} = 40 ms.

The NMR data were processed on a SGI 4D/25 workstation using FELIX 2.1 software (Biosym, San Diego, CA).

Distance Restraints and Molecular Modeling. The large majority of distance constraints for the structure calculations were determined from measurements of cross peak volumes in the 50-ms NOESY spectrum. The intramolecular drug and DNA peak volumes were then converted into strong, medium, and weak distance restraint categories. All lower bounds were set to 1.8 Å. Upper bounds were set to 3.0 Å for strong, 4.0 Å for medium, and 5.5 Å for weak restraints. The volume limits were established by a multiple calibration scheme, in which an effective calibration curve for the relationship between NOE volume and distance between protons is generated on the basis of the volumes for several different NOEs with distances that either are fixed or can vary by only very small amounts (*e.g.*, 1′H–2″H, 2′H–4′H). The categorization of the intermolecular drug–DNA peaks was based on the shortest mixing time at which they appeared in the NOESY spectrum, with 3.5-Å upper bounds at 50 ms, 4.5-Å at 100 ms, and 6.0-Å at 200 ms. Hydrogen bond restraints were enforced by constraining the N···O distance to 3.01–3.51 Å and the N···N distance to 3.05–3.55 Å for the G/C base pairs and the N···N distance to 2.92–3.42 Å for the A/T base pairs.

Starting structures were generated by manually docking calicheamicin θ_1^I (**1**) into standard A-DNA or B-DNA models with the d(GCATCCT-AGC)·d(GCTAGGATGC) sequence. Docking was carried out using INSIGHT II version 2.2 (Biosym). The molecular mechanics and dynamics refinements were performed either on a CRAY YMP/2E or a Convex C240 meta-cluster using the SANDER module of AMBER 4.1. The force constant for the distance restraint penalty function was 32 kcal/mol Å^2, the nonbonded cutoff was 9 Å, charges were scaled by 0.2, and a distance-dependent dielectric was utilized. The refiniments were initiated with 500 steps of restrained energy minimization, followed by a simulated annealing protocol consisting of the following steps: (a) 1 ps (1000 steps of 1 fs) of heating from 0 K to 750 K. The distance restraints were scaled by a factor of 0.1 at the beginning of this period and then slowly increased in strength to 32 kcal/mol Å^2; (b) 3 ps of equilibration at 750 K; and (c) 16 ps of slow cooling from 750 K to 0 K.

A cross-check on the accuracy of the upper distance bounds was made by back-calculating the NOESY spectrum from the structural models using the INTENSE subroutine contained in AMBER 4.1 and comparing the experimental and calculated cross-peak volumes.

Results and Discussion

The general strategies for sequence-specific assignment of the ^{1}H resonances of small DNA duplexes have been amply reviewed,[28] and the specific protocols used here for the free DNA and the drug–DNA complexes have been described.[29] The shorthand notation described by Wüthrich[28b] is used to specify DNA interproton distances and corresponding NOEs.

Scheme 2. Protocol Used for the Structure Calculation of the Model of the DNA–Calicheamicin θ_1^I Complex

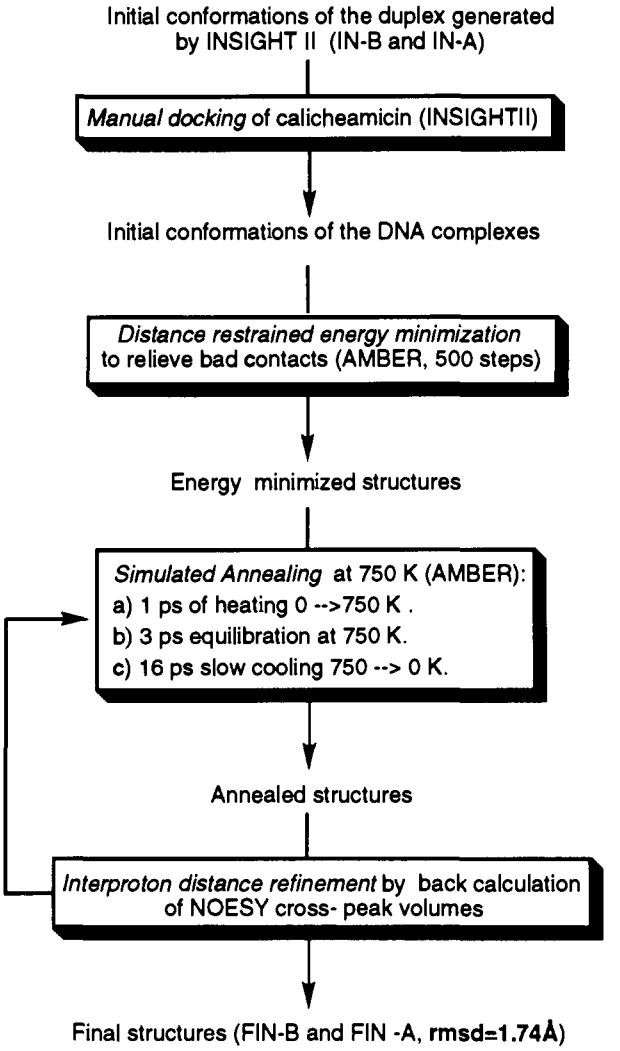

^{1}H NMR of the Free Duplex. All cytosine 5H–6H and thymine 5Me–6H resonances were readily identified by scalar connectivities in both 2QF-COSY and TOCSY spectra. All 20 1′H–2′H–2″H–3′H spin subsystems could be identified in the 2QF-COSY and TOCSY spectra and were confirmed by inspection of the NOESY spectra. The connectivity to 4′H resonances was obtained from NOESY spectra. The sequential resonance assignments were made in a short mixing time (50 ms) NOESY spectrum. The combination of $d_i(6,8;2')$, $d_s(2'';6,8)$, $d_i(5Me;6)$, and $d_S(6,8;5Me)$ connectivities were sufficient to obtain complete sequence-specific resonance assignments. The relative intensities of cross peaks [*e.g.*, $d_i(6,8;2')$, $d_S(2'';6,8) \gg d_i(6,8;2'')$, $d_s(2'';6,8)$ and $d_i(5Me;6) > d_s(6,8;5Me)$] in the same NOESY spectrum and the cross peak patterns in the 2QF-COSY spectrum clearly indicated that d(GCATCCTAGC)·d(GCTAGGATGC) is a B-form DNA duplex with predominantly $C_{2'}$-*endo* sugar conformations.

^{1}H NMR Assignments of the Ligand–DNA Complexes. Obtaining resonance assignments for the two ligand–DNA complexes proved much more difficult than for the free DNA, due to the fact that the line widths of nearly all DNA and drug ^{1}H resonances were significantly larger in the complex. The information content

(21) Marion, D.; Wüthrich, K. *Biochem. Biophys. Res. Commun.* **1983**, *113*, 500.
(22) Braunschweiler, L.; Bodenhausen, G.; Ernst, R. R. *Mol. Phys.* **1983**, *48*, 535.
(23) Rance, M.; Sorensen, O. W.; Bodenhausen, G.; Wagner, G.; Ernst, R. R.; Wüthrich, K. *Biochem. Biophys. Res. Commun.* **1983**, *117*, 479.
(24) Macura, S.; Ernst, R. R. *Mol. Phys.* **1980**, *41*, 95.
(25) Shaka, A. J.; Lee, C. J.; Pines, A. *J. Magn. Reson.* **1988**, *77*, 274.
(26) Plateau, P.; Guéron, M. J. *J. Am. Chem. Soc.* **1982**, *104*, 7310.
(27) Bothner-by, A. A.; Stephens, R. L.; Lee, J. T.; Warren, C. D.; Jeanloz, R. W. *J. Am. Chem. Soc.* **1984**, *106*, 811.
(28) (a) Wemmer, D. E.; Rels, B. R. *Annu. Rev. Phys. Chem.* **1985**, *36*, 105. (b) Wüthrich, K. *NMR of Proteins and Nucleic Acids*; Wiley: New York, 1986. (c) Patel, D. J.; Shapiro, L.; Hare, D. *Annu. Rev. Biophys. Chem.* **1987**, *16*, 423. (d) Reid, B. R. *Q. Rev. Biophys.* **1987**, *20*, 1.
(29) (a) Chazin, W. J.; Wüthrich, K.; Hyberts, S.; Rance, M.; Denny, W. A.; Leupin, W. *J. Mol. Biol.* **1986**, *190*, 439. (b) Chazin, W. J.; Rance, M.; Chollet, A.; Leupin, W. *Nucleic Acid Res.* **1991**, *19*, 5507. (c) Chen, S.; Leupin, W.; Rance, M.; Chazin, W. J. *Biochemistry* **1992**, *31*, 4406.

Table 1. Proton Chemical Shifts in the d(GCATCCTAGC)·d(GCTAGGATGC)–Calicheamicin θ_1^1 (1) Complex at pH 7.0, 293 K

DNA Chemical Shifts (ppm)[a]

residue	N_1H, N_3H	NH_2	2H, 5H, 5-Me	6H, 8H	1′H	2′H	2″H	3′H	4′H	5′H/5″H
G_1	*b*			7.86	5.87	2.51	2.68	4.80	4.18	3.63, 3.63
C_2		6.49, 8.34	5.35	7.40	5.50	2.05	2.38	4.82	4.08	
A_3			7.70 (7.82)[c]	8.30 (8.31)[c]	6.24	2.66	2.90	4.98	4.38	
T_4	13.23		1.30 (1.38)[c]	7.11 (7.14)[c]	6.17	2.00	2.72	4.84	4.15	
C_5		6.53, 8.02	5.38	7.22	5.91[d]	1.80	2.15	4.60	3.93	
C_6		6.53, 7.91	5.38	7.32	5.59[d]	1.84	2.49	4.51	4.51	
T_7	13.61		1.49	7.35	5.75	1.83	2.33	4.53	4.04	
A_8			7.86	8.13	6.00	2.65	2.80	4.98	4.35	4.06
G_9	12.85			7.61	5.73	2.38	2.53	4.89	4.29	
C_{10}			5.12	7.26	5.99	2.08	2.13	4.37	3.95	
G_{11}	b			7.88	5.91	2.57	2.68	4.80	4.20	3.66, 366
C_{12}		6.49, 8.18	5.29	7.47	5.96	2.04	2.40	4.73	4.14	
T_{13}	13.86		1.58	7.36	5.42	2.16	2.40	4.82	4.05	
A_{14}			7.88	8.09	6.21	2.62	3.01	4.99	4.38	
G_{15}	13.30	8.98, 9.69		7.53	5.30	2.45	2.60	4.89	4.32	
G_{16}	12.69			7.71	5.93	2.43	2.68	5.01	4.32	
A_{17}			7.76	7.95 (8.07)[c]	6.27	2.38	2.86	4.83	4.30	3.34, 306
T_{18}	13.40 (13.61)[c]		1.24 (1.12)[c]	6.82 (6.99)[c]	5.51	1.71	2.19	4.67	3.85	
G_{19}	12.81			7.76	5.86	2.49	2.62	4.89	4.21	4.02
C_{20}				7.34	6.07	2.03	2.15	4.44	3.98	

Calicheamicin θ_1^I (1) Chemical Shifts (ppm)[a]

sugar residue	H1	$H2_{ax}$	$H2_{eq}$	H3	H4	H5	Me	OMe	CH_3CH_2NH	5-OMe[e]	6-OMe[e]
A	4.55	3.52		4.32	2.33	3.84	1.29				
B	5.12	1.82	2.22	4.33	3.75	4.00	1.34				
C							2.43			3.75	4.01
D	5.19		4.55	3.91	3.58	4.21	1.36	3.60			
E	5.37	1.54	2.69	3.84	3.15	4.00		3.60	1.28, 3.00		

aglycone	H1	H4	H5	H9′	H9″	H14	*Me*CO
R	6.82	6.27 (6.04)[c]	6.27	3.26	2.84	6.2	2.18

[a] The chemical shifts are referenced to 3-(trimethylsilyl)propionic-2,2,3,3-d_4 acid, sodium salt, using the HOD resonance previously calibrated in stock buffer solution. [b] Not observed due to the rapid exchange with solvent at this temperature. [c] These resonances are doubled at this temperature. The chemical shifts in parentheses refer to the minor state of the complex. [d] Tentative assignments based solely on weak scalar connectivities observed in the TOCSY and 2Q spectra at 318 K. [e] For the calicheamicin θ_1^I (1) numbering, see Figure 1.

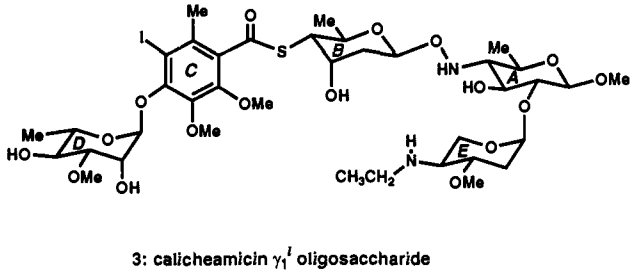

3: calicheamicin γ_1^I oligosaccharide

Figure 2. Structure of the oligosaccharide domain of calicheamicins θ_1^1 and γ_1^1 (methyl glycoside).

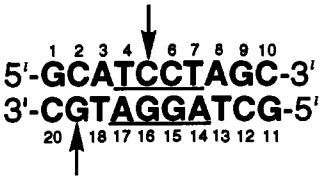

Figure 3. DNA sequence used in these studies. The recognition sequence is designated by underlines and the cleavage sites by arrows.

in the 2QF-COSY experiment was very limited, but 2Q and TOCSY experiments were much more informative because they are less sensitive to the cross peak cancellation associated with the larger line widths.

The acquisition of 2D NMR spectra over a range of temperatures proved important in the analysis of the two complexes because many key resonances could only be assigned at 318 K, where line widths were narrow, whereas most of the intermolecular NOEs could only be identified at 283 or 293 K. Once the assignments were obtained at 318 K, the spectra acquired at lower temperatures were reexamined and assignments transferred

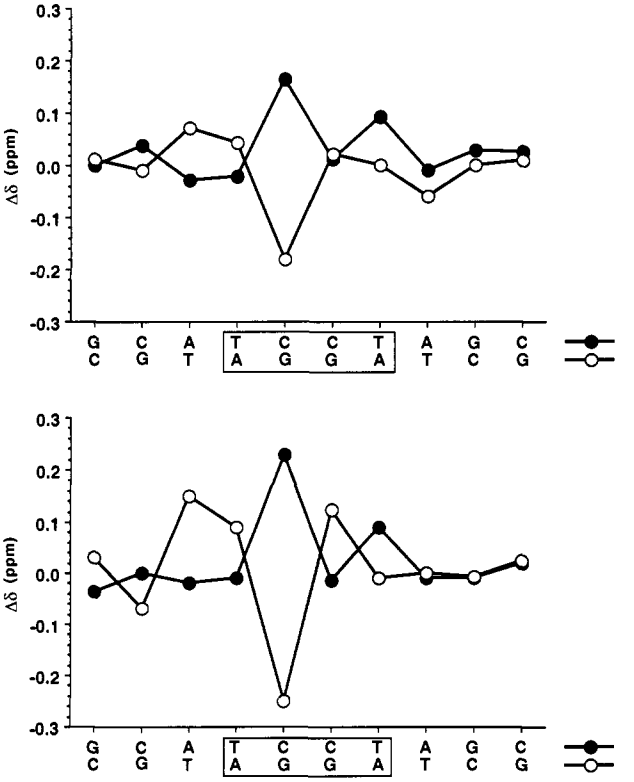

Figure 4. Chemical shift changes ($\delta_{free}-\delta_{bound}$) of the DNA 6H/8H protons (versus their location in the sequence) upon complexation with calicheamicin θ_1^I (1) (top) and with the oligosaccharide (3) (bottom). The DNA chemical shift perturbations induced by the binding of the intact calicheamicin θ_1^I and the oligosaccharide domain are very similar.

Table 2. Proton Chemical Shifts in the d(GCATCCTAGC)·d(GCTAGGATGC)–Calicheamicin Oligosaccharide (**3**) Complex at pH 7.0, 318 K

DNA Chemical Shifts (ppm)[a]

residue	N_1H, N_3H	NH_2	2H, 5H, 5-Me	6H, 8H	1′H	2′H	2″H	3′H	4′H	5′H/5″H
G_1	*b*			7.88	5.93	2.53	2.72	4.80	4.20	3.62, 3.62
C_2		6.34, 8.27	5.41	7.44	5.60	2.11	2.42	4.84	4.16	
A_3			7.70	8.31	6.31	2.70	2.98	5.03	4.40	
T_4	13.27		1.40	7.11	6.04	2.01	2.67	4.88	4.21	
C_5		6.49, 7.96	5.47	7.34	5.91[c]	1.77[c]	2.15[c]	4.70	3.93	
C_6		6.49, 7.81	5.44	7.38	5.66[c]	1.90	2.50	4.63	4.63	
T_7	13.48		1.58	7.33	5.74	1.91	2.38	4.72	4.10	
A_8			7.88	8.14	6.06	2.66	2.88	5.01	4.30	
G_9	12.74			7.56	5.74	2.39	2.58	4.91	4.33	
C_{10}			5.27	7.34	6.09	2.08	2.18	4.42	3.97	
G_{11}	*b*			7.91	5.96	2.60	2.79	4.80	4.20	3.62, 3.62
C_{12}		6.47, 8.18	5.39	7.49	6.02	2.08	2.46	4.77	4.20	
T_{13}	13.84		1.63	7.35	5.60	2.12	2.41	4.84	4.06	
A_{14}			7.91	8.11	6.13	2.62	2.95	5.01	4.34	
G_{15}	13.15	8.98		7.47	5.46	2.41	2.58	4.91	4.31	
G_{16}	12.54			7.78	5.91	2.40	2.67	5.01	4.33	
A_{17}			7.70	8.04	6.30	2.45	2.91	4.89	4.32	3.04, 3.29
T_{18}	13.27 (13.49)[d]		1.30	6.91	5.51	1.83	2.31	4.81	3.95	3.87
G_{19}	12.69			7.79	5.90	2.55	2.66	4.95	4.32	
C_{20}			5.38	7.41	6.16	2.12	2.20	4.46	4.03	

Oligosaccharide (**3**) Chemical Shifts (ppm)[a]

residue	H1	$H2_{ax}$	$H2_{eq}$	H3	H4	H5	Me	OMe	CH_3CH_2NH	5-OMe[e]	6-OMe[e]
A	4.22	3.26		4.32	2.39	3.90	1.42	3.58			
B	5.16	1.95	2.26	4.37	3.74	4.07	1.41				
C							2.43			3.81	4.01
D	5.28		4.61	3.95	3.60	4.17	1.36	3.60			
E	5.29	1.63	2.74	3.90	3.21	3.96, 4.02		3.60	1.28, 3.06		

[a] The chemical shifts are referenced to 3-(trimethylsilyl)propionic-2,2,3,3-d_4 acid, sodium salt, using the HOD resonance previously calibrated in stock buffer solution. [b] Not observed due to the rapid exchange with solvent at this temperature. [c] Tentative assignments based solely on weak scalar connectivities observed in the TOCSY and 2Q spectra. [d] This resonance is doubled at 283 K. [e] For the oligosaccharide (**3**) numbering, see Figure 2.

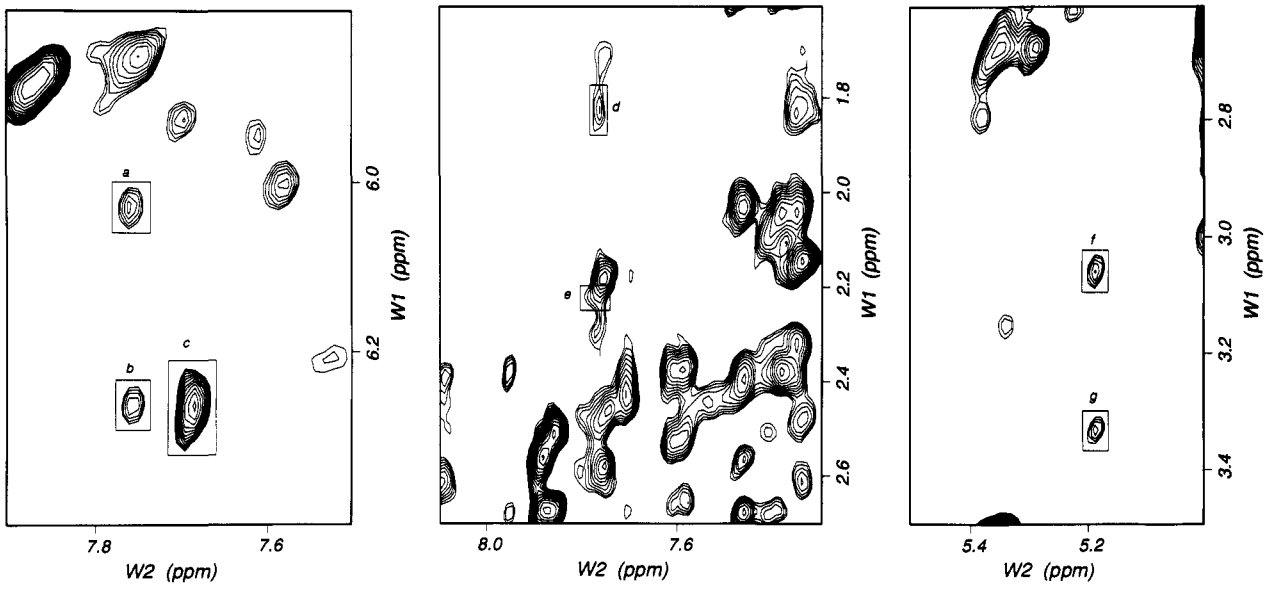

Figure 5. Expanded regions of the 500-MHz NOESY spectrum (τ_m = 300 ms, T = 293 K) of the calicheamicin θ_1^I (**1**)–DNA complex, containing selected intermolecular NOEs. (a) R-4H/A_{17}-2H; (b) R-4H/A_{17}-2H; (c) R-5H/A_3-2H; (d) B-2_{ax}H/A_{17}-2H; (e) B-2_{eq}H/A_{17}-2H; (f) D-1H/A_{17}-5′H; (g) D-1H/A_{17}-5″H.

in a stepwise manner. This strategy allowed nearly complete characterization of the two complexes at 283, 293, and 318 K. It is remarkable that for residues C_5 and C_6, no 6H/1′H NOESY cross peaks could be identified over the whole range of temperatures. A tentative assignment for the 1′H of both C_5 and C_6 was obtained from a weak cross peak observed only in the TOCSY experiment at 318 K. The absence of these scalar and dipolar connectivities is attributed to the large line widths of these resonances. An inspection of the relative intensities of cross peaks in the 50-ms NOESY spectrum indicated that upon binding of the drug, the duplex retains B-form geometry with predominantly $C_{2'}$-*endo* sugar conformations. The ^1H resonance assignments for calicheamicin θ_1^I (**1**) and oligosaccharide (**3**, Figure 2) molecules in their respective complexes were made from 2QF-COSY and TOCSY spectra, aided by the assignments available for the free compounds in CD_3OD. The sequence-specific ^1H NMR assignments for the drug and DNA resonances in the calicheamicin θ_1^I–DNA complex are listed in Table 1, while those for the oligosaccharide–DNA complex are listed in Table 2.

DNA and Calicheamicin θ_1^I Complexation Shifts. The analysis of the changes in the DNA proton chemical shifts induced by drug binding provides important insight into the regions of contact

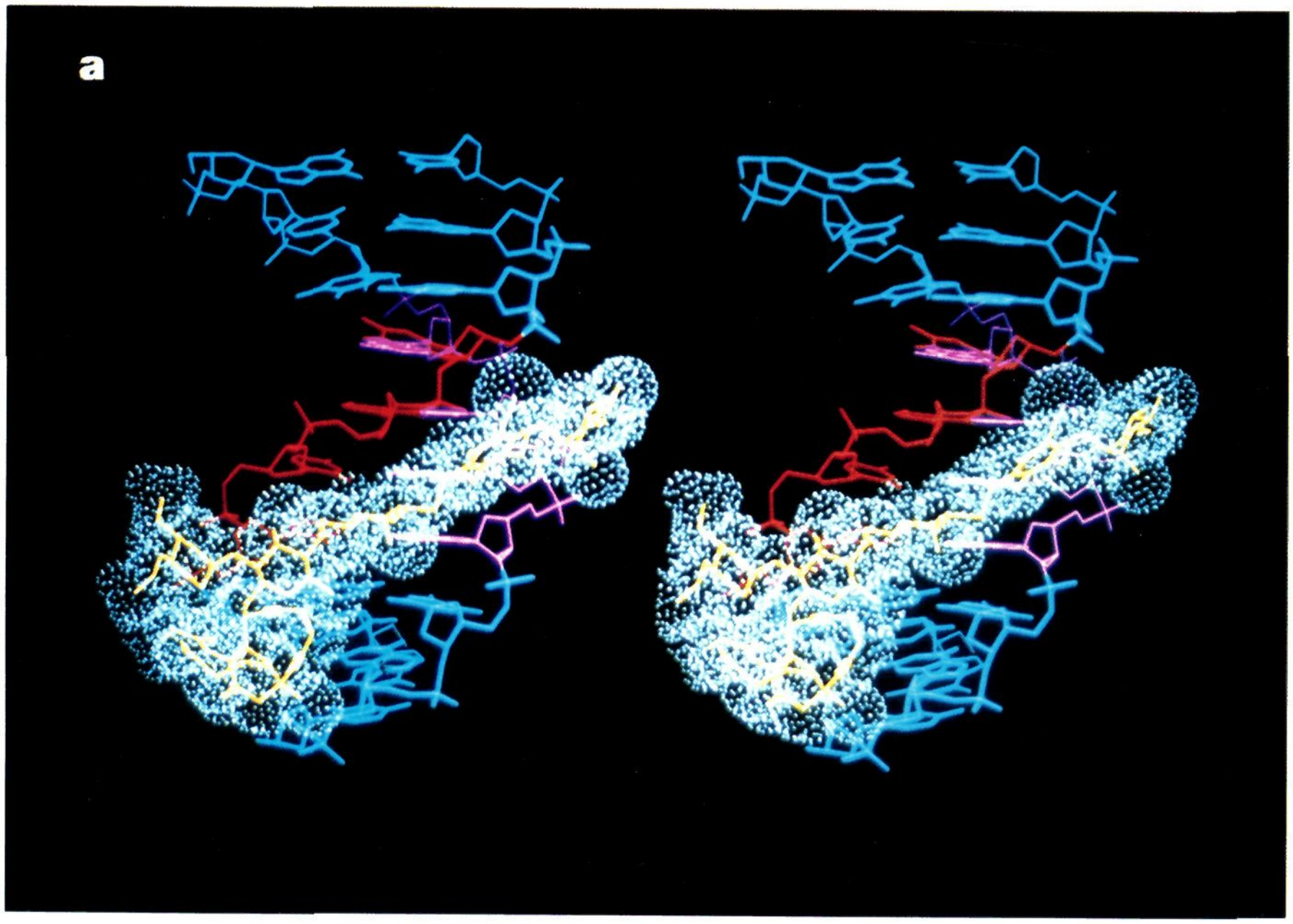
a

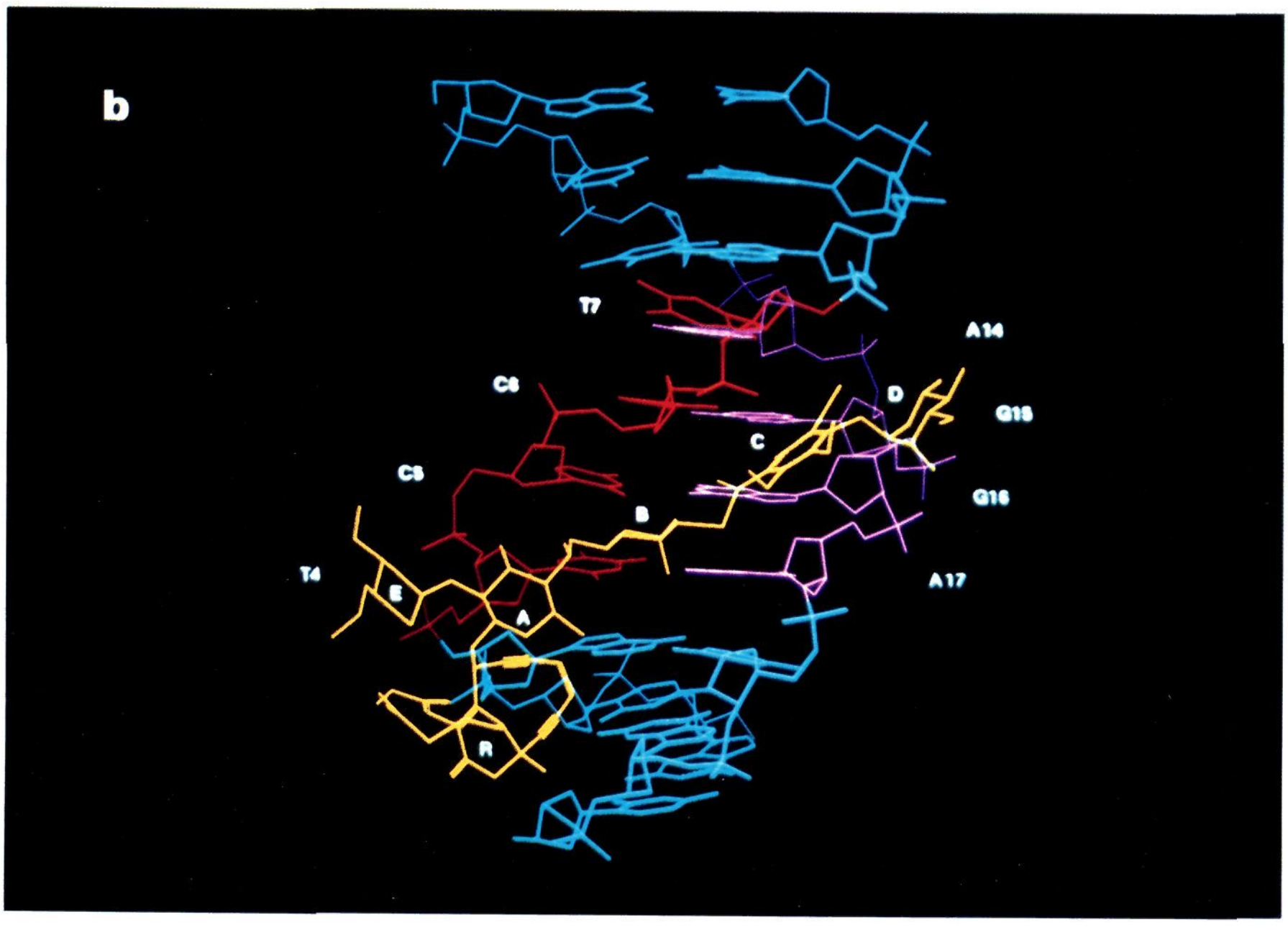
b
T7
A14
C8
D
G15
C
C5
G16
B
T4
A17
E
A
R

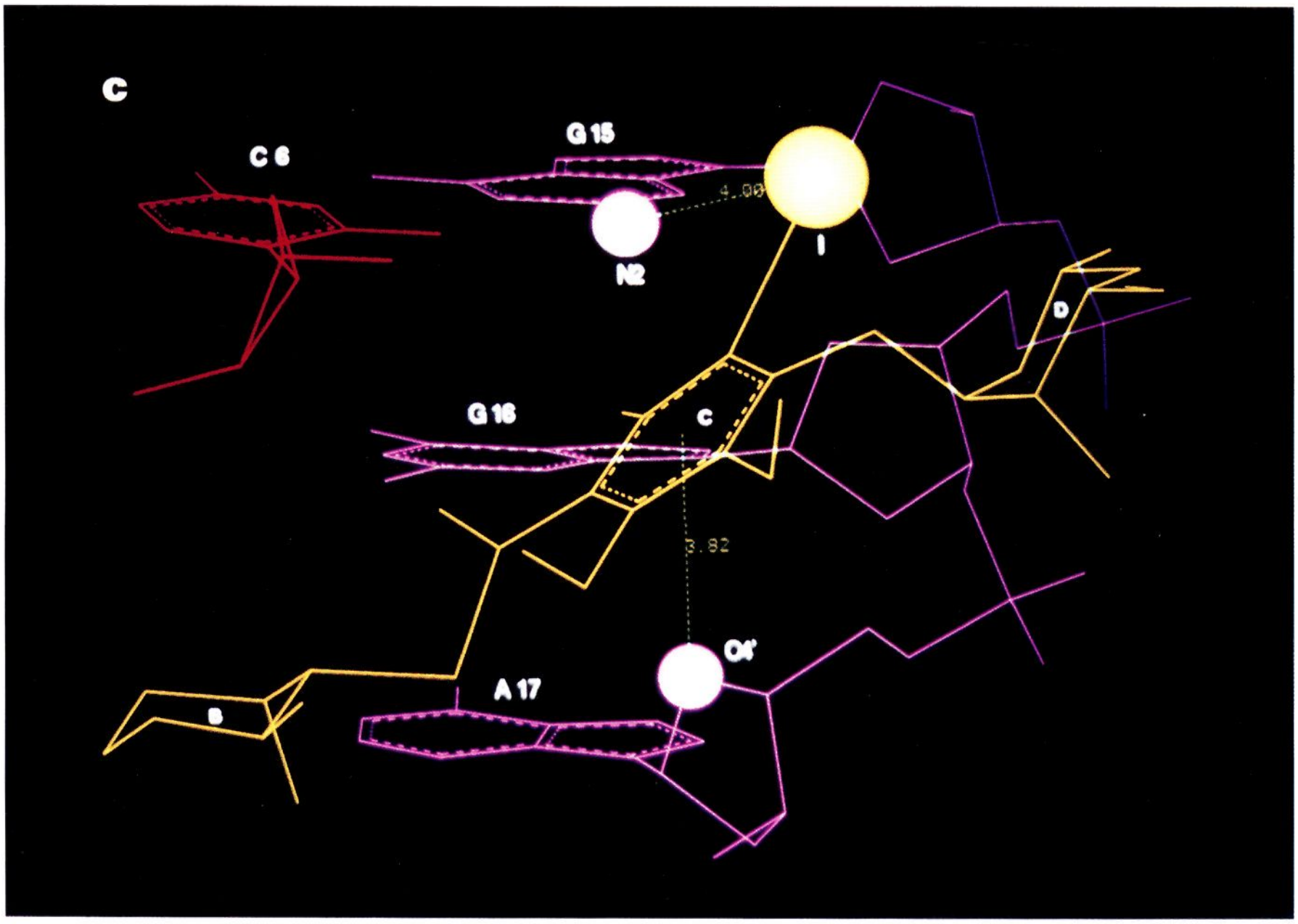

Figure 6. (a) Stereoview of the model of the calicheamicin θ_1^I (**1**)–DNA complex. The drug is shown in yellow, with the TCCT and AGGA tracts in red and purple, respectively. The van der Waals surface of calicheamicin θ_1^I is displayed in white dots. (b) Wireframe model of calicheamicin θ_1^I (**1**)–DNA complex. The drug residues and the DNA residues belonging to the recognition site are labeled. (c) Expanded region of the same structural model showing the interactions of the drug aromatic ring C with DNA. The iodine atom and the G_{15} amino nitrogen are displayed as spheres. The stacking interaction between the ring C and the A_{17} ring oxygen is also shown (see text).

between the two molecules in the complex. The DNA sequence used in these studies is shown in Figure 3. A plot of $\Delta\delta$ ($\delta_{free}-\delta_{bound}$) for the DNA base protons (6H/8H) versus location in the sequence is shown in Figure 4 (upper panel). Significant shifts are observed for the residues from C_5 to T_7 in the TCCT strand and from G_{15} to T_{18} in the AGGA strand, while weaker effects extend one or two base pairs beyond these nucleotides. The strongest chemical shift perturbation occurs at the C_5/G_{16} base pair.

The evaluation of the changes in proton chemical shift upon binding to DNA was complicated by the fact that no NMR data in D_2O are available for the free calicheamicin θ_1^I, due to the very poor water solubility of this compound. However, a comparison of the chemical shifts of the free drug in CD_3OD with those of the bound drug in D_2O reveals no substantial differences, strongly suggesting that the drug does not undergo dramatic conformational changes upon binding.

The Role of the Calicheamicin Oligosaccharide Domain. The binding of the calicheamicin oligosaccharide (**3**) to DNA has been investigated by footprinting experiments.[8] Our recent kinetic experiments have provided binding constants for calicheamicin γ_1^I (**2**) and of a number of derivatives of the oligosaccharide **3** and showed that the presence of the aglycone increases the affinity of the sugar toward DNA.[10] The present study includes a complementary and detailed comparative analysis of the NMR parameters observed for the oligosaccharide (**3**) and intact calicheamicin. The ligand-induced changes in the chemical shifts ($\Delta\delta$) of the DNA protons have been carefully examined for both complexes. The plots for the base protons (6H/8H) are compared in Figure 4. These $\Delta\delta$ data indicate that the effects induced by the binding of the intact calicheamicin molecule and of the sugar **3** alone are very similar. This conclusion is further supported by an extensive analysis of cross peaks in NOESY spectra acquired for the two complexes under identical conditions, which reveals that their patterns of intermolecular contacts are virtually identical (Tables 3 and 4). Even the slow rate of solvent exchange of the G_{15} amino protons and the unique low-field chemical shift (9.80 ppm) of one of these resonances (*vida infra*) is faithfully reproduced in the oligosaccharide–DNA complex. Taken together, these data provide strong evidence that the calicheamicin sugar binds and interacts with duplex DNA in a manner that is largely independent of the presence of the aglycone. This implies that the primary structural determinants for binding and the basic elements for sequence specificity of calicheamicin are due to the oligosaccharide portion. The increased affinity of the intact calicheamicin may be attributed to the lipophilic character of the aglycone, although more specific interactions cannot be excluded at this time.

Structural Model of the DNA–Calicheamicin θ_1^I Complex. A number of intermolecular cross peaks are detected in the NOESY spectra of the calicheamicin–DNA complex (*e.g.*, Figure 5), thereby providing direct evidence of drug binding. All unambiguously assigned intermolecular NOEs are listed in Table 3. In addition to this, several other drug–DNA NOE cross peaks were clearly observable but could not be assigned with certainty owing to the severe resonance overlap in some regions of the ^1H spectrum. All of the residues of calicheamicin, except for the amino sugar E, make direct contacts with the DNA. The DNA

Table 3. Drug–DNA Intermolecular NOEs Observed for the 1:1 Complex d(GCATCCTAGC)·d(GCTAGGATGC)–Calicheamicin θ_1^1 (**1**) at 293 K

proton 1 (drug)	proton 2 (DNA)	size[a]	proton 1 (drug)	proton 2 (DNA)	size[a]
R-H4	A_{17}-2H	w	C-90Me	A_{17}-5″H	w
R-H5	A_3-2H	s	D-H1	A_{17}-5′H′	s
A-Me	G_{19}-4′H	m	D-H1	A_{17}-5″H	s
B-Me	C_6-4′H′	s	D-H2	A_{17}-5′H	s
B-$H2_{ax}$	A_{17}-2H	m	D-H2	A_{17}-5″H	s
B-$H2_{eq}$	A_{17}-2H	m	D-OMe	G_{16}-4′H	m
B-$H2_{eq}$	G_{16}-1H	w	D-OMe	G_{15}-2H	w
C-90Me	A_{17}-5′H	w			

[a] w = weak, m = medium, s = strong, based on the shortest mixing time at which these NOEs first appear: strong at τ_m = 50 ms, medium at τ_m = 100 ms, and weak at τ_m = 200 or 300 ms.

Table 4. Oligosaccharide–DNA Intermolecular NOEs Observed for the 1:1 Complex d(GCATCCTAGC)·d(GCTAGGATGC)–Calicheamicin Oligosaccharide (**3**) at 293 K

proton 1 (oligosaccharide)	proton 2 (DNA)	size[a]	proton 1 (oligosaccharide)	proton 2 (DNA)	size[a]
A-Me	G_{19}-4′H	s	B-H3	G_{16}-1H	w
B-Me	C_6-4′H′	s	D-H1	A_{17}-5′H	s
B-H1	T_{18}-4′H′	s	D-H1	A_{17}-5″H	s
B-H1	T_{18}-H5′	s	D-H2	A_{17}-5′H	s
B-$H2_{ax}$	A_{17}-2H	m	D-H2	A_{17}-5″H	s
B-$H2_{eq}$	A_{17}-2H	m	D-OMe	G_{16}-4′H	m
B-$H2_{eq}$	G_{16}-1H	w	D-OMe	G_{15}-2H	w
B-H3	A_{17}-2H	s			

[a] w = weak, m = medium, s = strong, based on the shortest mixing time at which these NOEs first appear: strong at τ_m = 50 ms, medium at τ_m = 100 ms, and weak at τ_m = 200 or 300 ms.

Table 5. Drug–Drug Interresidue NOEs Observed for the 1:1 Complex d(GCATCCTAGC)·d(GCTAGGATGC)–Calicheamicin θ_1^1 (**1**) at 293 K[a]

proton 1	proton 2	size[b]	proton 1	proton 2	size[b]
R-H1	E-$H5_{ax}$	m	A-Me	B-H1	m
R-H1	A-H1	s	B-Me	C-90Me[b]	s
R-H4	A-Me	m	D-Me	C-80Me[b]	s
E-H1	A-H2	s	D-H1	C-90Me[b]	s
A-Me	B-$H2_{ax}$	w			

[a] These NOEs were observed in a 50-ms NOESY spectrum (T = 293 K). [b] w = weak, m = medium, s = strong. This categorization is based on the volume of the cross peaks.

protons involved in these contacts include 4′H, 5′H, 5″H, and adenine 2H of residues A_3-C_6 and G_{15}-A_{17}, all located in the minor groove of the DNA duplex. A similar pattern of drug–DNA contacts has been reported by Kahne and co-workers,[18] although some differences exist due to the differences in the DNA sequence.

The first step toward producing a structural model for the drug–DNA complex involved the generation of two initial structures by docking the ligand onto duplex models of d(GCATCCTAGC)·d(GCTAGGATGC) in standard B-DNA (IN-B) and A-DNA (IN-A) conformations. The initial conformation of calicheamicin was generated using the interresidue NOEs observed for the drug in the bound state (Table 5). The drug was subjected to restrained energy minimization and then manually docked onto the preminimized duplexes so that all of the intermolecular NOEs were visually satisfied. The complex was then energy minimized to relieve bad van der Waals contacts. For subsequent steps, the 2′H and 2″H atom labels had to be switched in the PDB output file because their stereochemical assignment was reversed in the DNA structures generated by our version (2.2) of INSIGHT II.

The second step in generating structural models involved restrained molecular dynamics calculations using the SANDER module of AMBER 4.1. Two new atom types were created for the alkene and alkyne carbons in the enediyne portion of calicheamicin. The equilibrium bond lengths and bond angles of calicheamicin that are not present in the standard AMBER libraries were derived from *ab initio* calculations. The parameters obtained were in good agreement with those reported by Walker *et al.*[30] Force constants were determined by the method of interpolation as described by Weiner *et al.*[31] Partial charges for calicheamicin were obtained by MOPAC calculations (AM-1 program) assuming a total charge of +1. Reduced DNA phosphate charges and a distance-dependent dielectric were used to take into account the absence of counterions and explicit water molecules in the simulation. A lone pair had to be added to the chiral nitrogen of the N–O glycosidic linkage of calicheamicin to prevent its inversion during the molecular dynamics calculations.

The two starting structures were reminimized in the AMBER force field and then subjected to the simulated annealing protocol outlined in Scheme 2. At the end of the first round of refinement, the structural models were used to back-calculate NOESY cross peak volumes using the INTENSE routine in the AMBER. The calculated volumes were then compared to the experimental volumes, and peaks with volumes that were higher in the experimental spectrum than in the back-calculated spectra (*i.e.*, those that were overconstrained) were put into the next higher distance bound category. Restraints that were stronger in the theoretical spectra were left in the same category. A few typographical errors were also identified by this procedure. The modified restraint list was then used for a new round of refinement using the same two starting structures.

After the second round of refinement, no distance restraint violations >0.2 Å were present. A best-fit superimposition of the structures FIN-B and FIN-A produced from IN-B and IN-A provided a root mean square deviation (rmsd) for all atoms of 1.74 Å. The ring E and the two side chains of the aglycone portion of calicheamicin are the least well-defined regions of the complex, as they are at the surface, do not contact the DNA, and are restrained only by few interresidue NOEs. In general, the phosphodiester backbone, for which no direct experimental NMR data are available, is also poorly defined. The structure is best defined at the central d(ATCCT)·d(TAGGA) regions, where the drug is located and thus the NOE density is highest. The all-atom rmsd for this region of the complex is 1.12 Å. The refined structure derived from IN-B (B-DNA) is used for subsequent analysis because the IN-A structure, while very similar to the IN-B structure, has boat conformations for the A and E rings of the drug (*vide infra*).

A wireframe model of the calicheamicin–DNA complex is presented in Figure 6. After refinement, the DNA duplex remains in the B-DNA family, although local variations are observed. The deoxyribose rings are predominantly in a $C_{2'}$-*endo* conformation, except for the residues T_{18} and C_5 which possess a $^3T_2$ twisted conformation. The width of the minor groove, as indicated by the interstrand phosphorus–phosphorus distance, is 5–6 Å in standard B-DNA duplexes as opposed to ~11 Å in standard A-DNA. In the complex, groove width is largest at the binding site, ranging from 7.1 to 8.5 Å, with the expansion presumably due to accommodation of the drug.

The conformation of the bound calicheamicin is clearly evident in Figure 6b. All of the 6-membered rings of the drug are in chair conformations, consistent with the pattern of intraresidue NOEs observed for each ring and the multiplet structure of cross peaks in the DQF-COSY spectrum of the complex. The strong NOEs between the D-Me and C-5-OMe and between C-6-OMe and B-Me (Table 5) are crucial to defining the conformation around the B–C and C–D linkages. Thus, the two methoxy groups

(30) Walker, S.; Gupta, V.; Kahne, D.; Gange, D. *J. Am. Chem. Soc.*, in press.

(31) Weiner, S. J.; Kollman, P. A.; Case, D. A.; Singh, U. C.; Ghio, C.; Alagona, G.; Profeta, S.-J.; Weiner, P. *J. Am. Chem. Soc.* **1984**, *106*, 765.

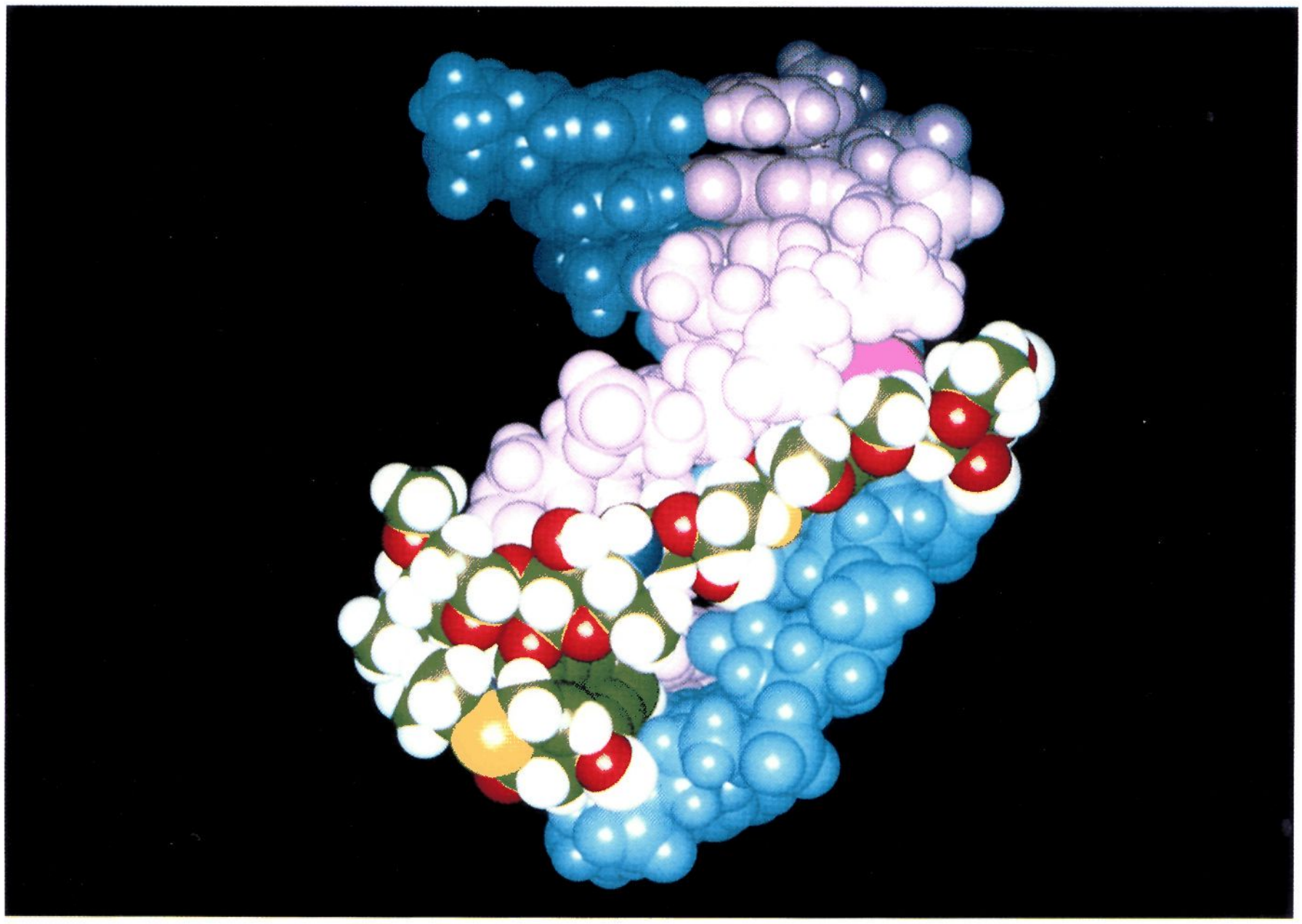

Figure 7. CPK model of the calicheamicin θ_1^I (**1**)–DNA complex. The DNA atoms are displayed in light blue (AGGA strand) and pink (TCCT strand). The drug atoms are displayed in different colors according to the atom type (carbon, green; hydrogen, white; nitrogen, blue; oxygen, red; sulfur, yellow; and iodine, purple).

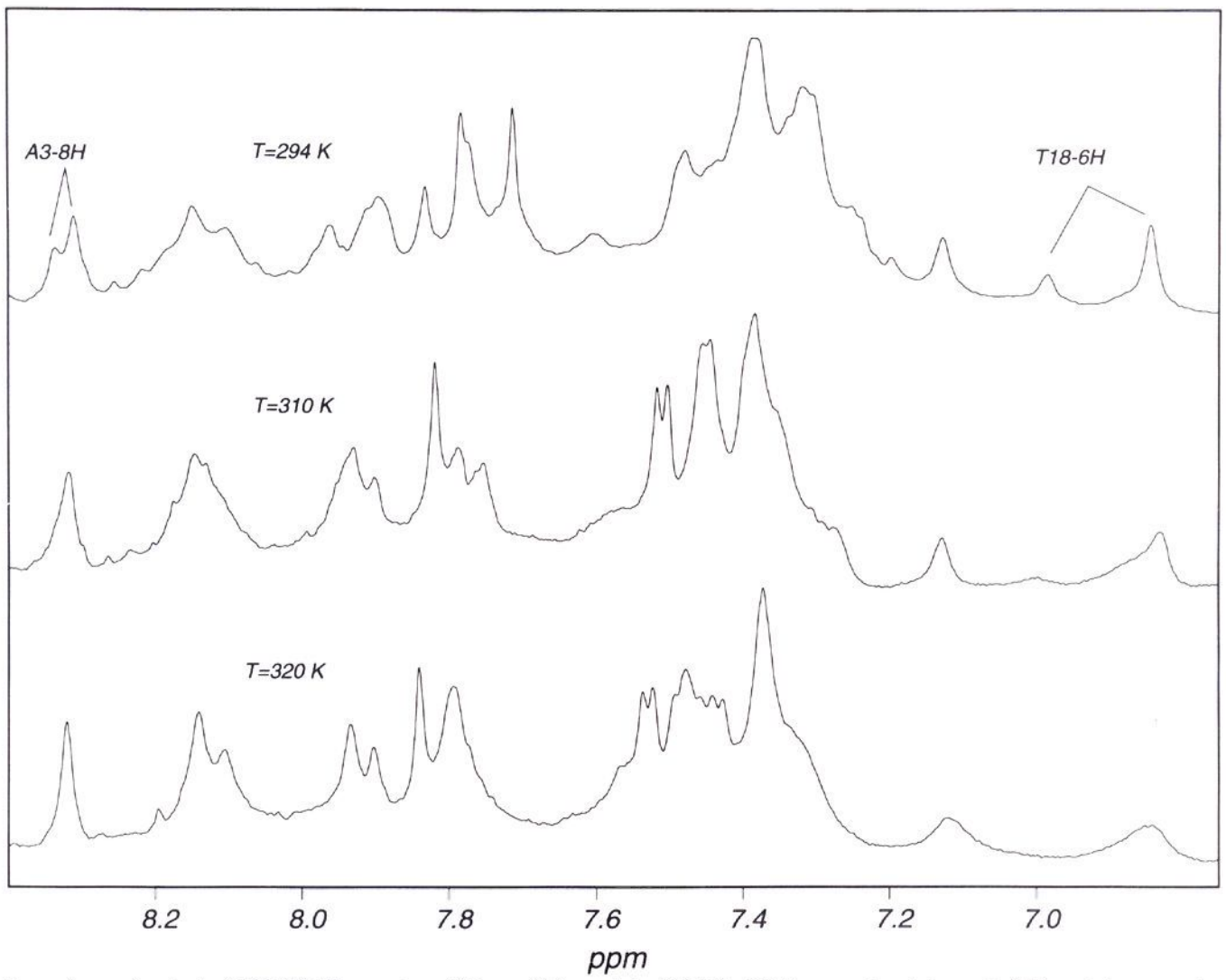

Figure 8. Aromatic regions of selected ^{1}H NMR spectra of the calicheamicin θ_1^I (**1**)–DNA complex taken at different temperatures. At and below 294 K, both A_3-8H and T_{18}-6H protons are clearly in slow exchange. From 305 K to 310 K, the peaks coalesce, and they completely merge in the range 315–320 K.

Table 6. Drug–DNA Intermolecular H-Bonds[a] Observed in the Structural Model for the d(GCATCCTAGC)·d(GCTAGGATGC)–Calicheamicin θ_1^I (1) Complex

donor	acceptor	donor	acceptor
R-8*OH*	G_{19}-*O3'*	G_{16}-*NH*$_2$	C-SC=*O*
B-3*OH*	A_{17}-*N*3	D-2*OH*	A_{17}-*O*1P

[a] The H-bonds are defined on the basis of a distance cutoff of 3.0 Å.

of the C ring and the two methyl groups of the B and D rings are all on the same side of the molecule. Four interresidue NOEs are critical to orienting the aglycone relative to rings A, B, and E: the strong NOEs, A-H2/E-H1 and A-H1/R-H1, and two weaker NOEs, A-Me/B-H1 and A-Me/B-H2$_{ax}$. These NOEs also serve to constrain the N–O linkage which connects rings A and B. The shape of the molecule is characterized by a gentle curvature in the sugar portion, which is very common to molecules that bind in the DNA minor groove.

A CPK model of the B-DNA structure of the DNA–calicheamicin θ_1^I complex is displayed in Figure 7. This model clearly shows the van der Waals complementarity between calicheamicin and the duplex (see also Figure 6a). The crescent shape of the oligosaccharide domain maximizes favorable interactions with the DNA duplex by following the curvature of the minor groove. The very unusual N–O linkage between rings A and B is a critical element of calicheamicin,[30] which seems to be crucial to this shape complementarity. The final refined structure has a substantial negative van der Waals energy (Lennard-Jones potential), indicating the absence of any unfavorable contacts in the proposed structure. Indeed, the van der Waals interactions must play an important role in the formation of DNA-calicheamicin complexes, due to the highly lipophilic character of the drug.

The location of the six calicheamicin residues with respect to the DNA duplex is best illustrated in the wireframe model shown in Figure 6b. The aglycone moiety (R), which contains the enediyne functionality responsible for the DNA cleavage, contacts the DNA in the region of the A_3/T_{18} and T_4/A_{17} base pairs. The 6-deoxypyranose rings A and B are proximate to the T_4/A_{17} and C_5/G_{16} base pairs. The amino sugar E, attached to the C-2 position of residue A, lies outside of the minor groove. The hexasubstituted aromatic ring C occupies a position between the two guanine resiudes G_{15} and G_{16} and appears to be closer to the AGGA strand than to the TCCT tract. Part of sugar residue D is actually outside the DNA minor groove, while the carbons C-1 and C-2 and the ring oxygen are in close proximity to the phosphate backbone of the AGGA strand, consistent with the presence of DNA 5'H and 5''H intermolecular NOEs.

In-depth analysis of the structure reveals that binding of the drug is stabilized by several specific interactions. The aromatic ring C stacks with the deoxyribose ring oxygen of the A_{17} and, to a lesser extent, with the ring oxygen of G_{16} (Figure 6c). This type of stacking interaction between aromatic rings and sugar oxygen atoms has been observed in other drug–DNA complexes.[32-34] The complex is also stabilized by four intermolecular hydrogen bonds (Table 6). Furthermore, there are strong indications of a salt bridge formed between the positively charged nitrogen of the ethylamino group of calicheamicin ring E and the phosphate oxygen of C_5, although there is no direct experimental evidence for this interaction from the NMR data. However, the absence or presence of this salt bridge in solution cannot be established from the current model, since the refinements have been carried out *in vacuo*.

(32) (a) Pelton, J. G.; Wemmer, D. E. *Biochemistry* **1988**, *27*, 8088. (b) Coll, M.; Frederick, C. A.; Wang, A. H.-J.; Rich, A. *Proc. Natl. Acad. Sci. U.S.A.* **1987**, *84*, 8385.
(33) Kopka, M. L.; Yoon, C.; Goodsell, D.; Pjura, P.; Dickerson, R. E. *J. Mol. Biol.* **1985**, *183*, 553.
(34) Pjura, P. E.; Grzeskowiak, K.; Dickerson, R. E. *J. Mol. Biol.* **1987**, *197*, 257.

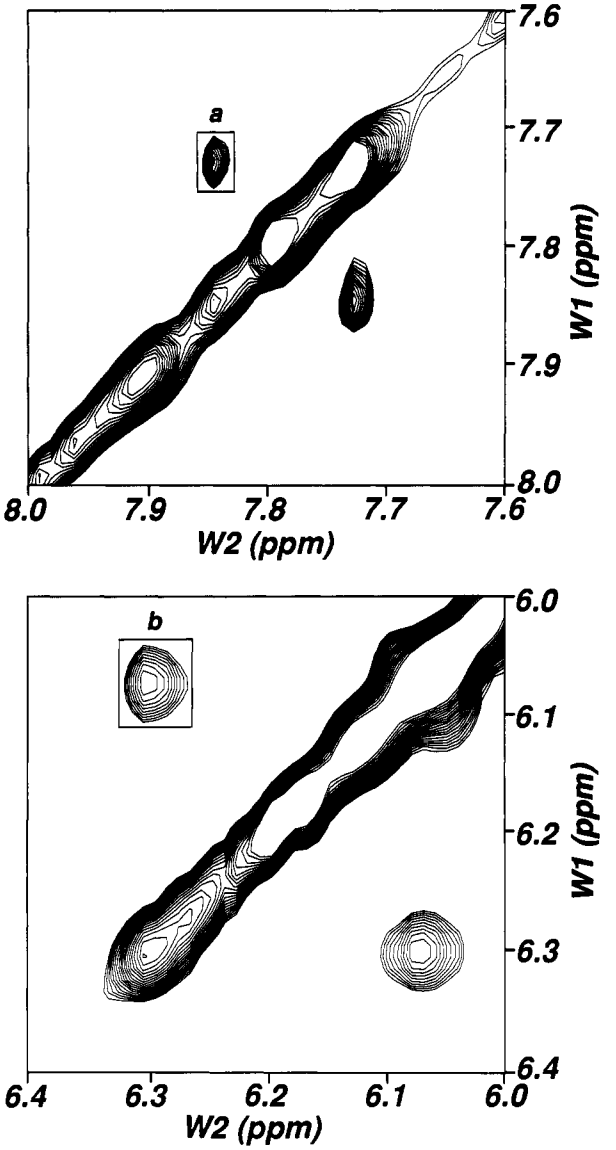

Figure 9. Expanded regions of the 500-MHz NOESY spectrum (τ_m = 800 ms, T = 294 K) of the calicheamicin θ_1^I (1)–DNA complex. The cross peaks in the boxes arise from chemical exchange between the two binding modes: (a) A_3-2H; (b) R-4H.

Among the labile protons of the DNA, the G_{15} amino protons display a striking behavior. Both of these resonances are relatively narrow and significantly downfield shifted to 8.98 and 9.69 ppm. The observation of relatively sharp, low-field resonances for guanosine amino protons is very unique and indicates that their exchange rate is considerably slower than usual. Since this phenomenon is not detected for any of the other guanine amino protons of the DNA in the complex or in the free duplex, we conclude that the drug binding must induce this behavior. In fact, residue G_{15} is located directly in the calicheamicin binding site. Figure 6c shows the location of the aromatic ring C of calicheamicin within the vicinity of the residue G_{15} and with the iodine atom pointing in the direction of the G_{15} amino group. The deshielding ring current of the aromatic system C can account for the unusual chemical shift observed for the two G_{15} amino protons, while the steric hindrance provided by the nearby iodine atom may be responsible for the reduction in the rate of rotation around the C_2–N_2 bond. Kinetic studies[10] on the binding properties of several calicheamicin oligosaccharide derivatives with H, CH_3, F, Cl, and Br atoms replacing the iodine atom of ring C[10] have demonstrated that these compounds have different affinities for DNA [using d(TCCT) as binding site]. In

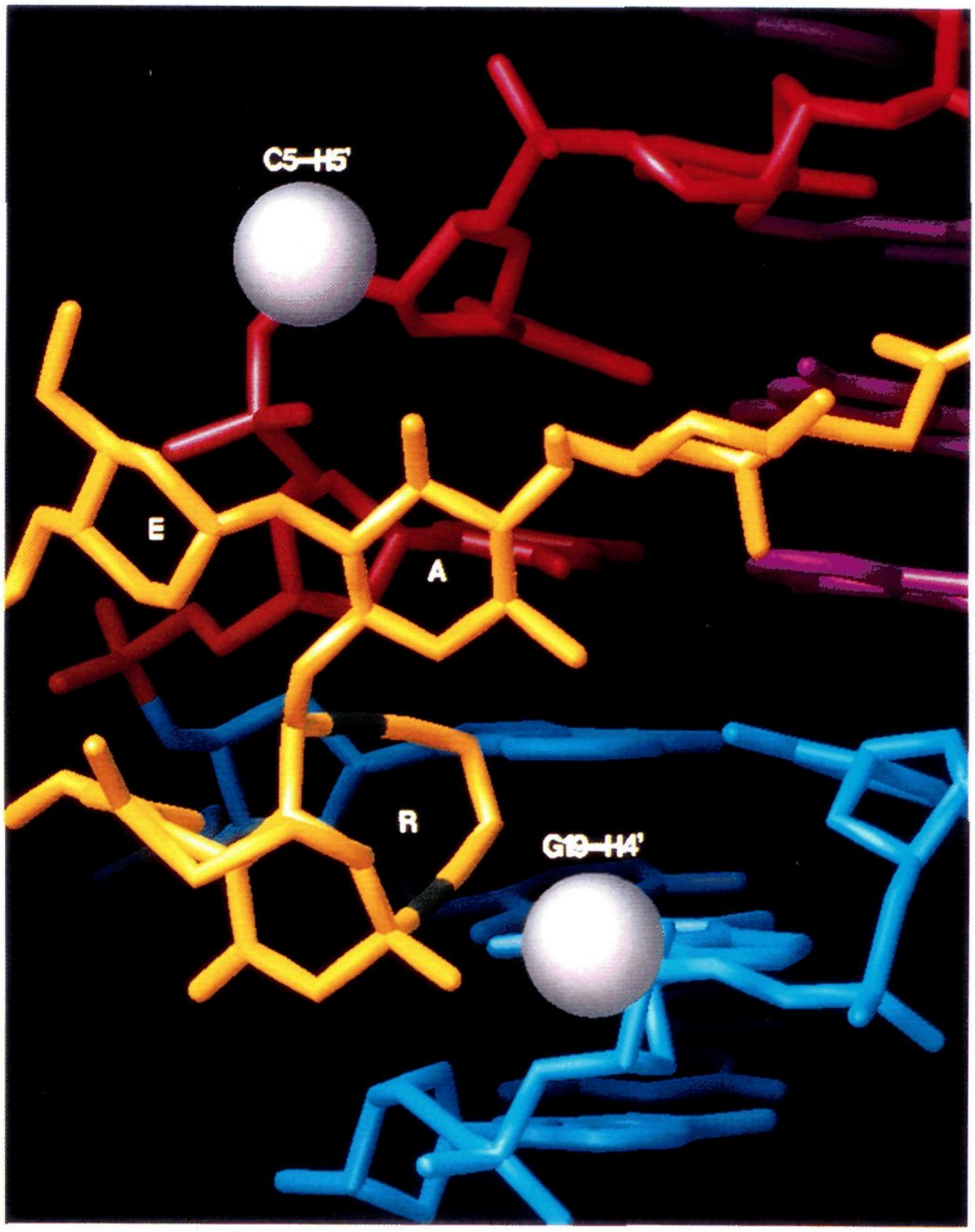

Figure 10. Expanded region of the structural model of the calicheamicin θ_1^I (**1**)–DNA complex. The color code is the same as in Figure 6. The hydrogen atoms (C_5-5′H and G_{19}-4′H) abstracted by the activated form of calicheamicin are displayed as white spheres. In this model, the aglycone is located closer to the G_{19} abstraction site on the AGGA strand than to the C_5 site on the TCCT strand, suggesting that DNA cleavage requires a dynamic process with the aglycone moving within the minor groove (see text).

particular,[10] the binding constant is highest for the iodine sugar and decreases following the order I > Br > Cl > Me > F ≫ H. There is a fairly good correlation[10] between the binding constant of these derivatives and the atomic radius of the substituents, suggesting that steric effects may be important in this regard, although the weak binding of the Me sugar seems to be out of order. In addition to steric effects, one must assume that van der Waals and/or electrostatic interactions must also play an important role.

Dynamics of the DNA–Calicheamicin θ_1^I Complex. Upon lowering of the temperature below 300 K, several broad drug and DNA resonances in the ^{1}H NMR spectra of the 1:1 complex split in two discrete resonances in a ratio of *ca.* 3.2:1 (Figure 8). The molar ratio of calicheamicin and DNA in the complex was carefully monitored during titration; hence this phenomenon is attributed to the presence of two unequally populated species in solution. Since a coalescence phenomenon is observed upon raising the temperature, these discrete species must arise from slow interconversion between two low-energy conformational substates. A similar observation has been made for the d(GTGACCTG)·d-(CAGGTCAC)–calicheamicin complex,[18] although the difference in population of the two states was more than two-fold greater (*ca.* 8:1).

The characterization of this chemical exchange phenomenon was carried out by carefully examining the temperature dependence of the ^{1}H NMR spectrum (273–330 K) and by acquiring ROESY and long mixing time NOESY experiments. Selected 1D ^{1}H NMR spectra of the aromatic proton region are shown in Figure 8, illustrating the temperature-dependent coalescence of resonances. Figure 9 shows expanded regions from the 800-ms NOESY spectrum of the complex, which contain exchange cross peaks between resonances from the major and minor species for one drug (b) and one DNA (a) proton. The largest chemical shift difference between corresponding resonances from the major and minor species is observed for the 6H of T_{18} ($\Delta\nu$ = 80 Hz), which coalesce at 320 K. Most of the other doubled resonances have considerably smaller chemical shift differences and correspondingly lower coalescence temperatures (305–310 K). A

lower limit for the rate of exchange at coalescence can be determined from the limiting chemical shift differences measured in the slow exchange regime.[35] From $\Delta\nu$ for T_{18}-6H, the values at 320 K are $k_{maj} > 5.2 \times 10^1$ s^{-1} and $k_{min} > 1.6 \times 10^2$ s^{-1}, corresponding to an upper limit on the lifetimes of 19 and 6 ms, respectively. An estimate of the activation energy ($\Delta G^{\ddagger}$) for this phenomenon can be made from the value of the coalescence temperature and the limiting chemical shift difference, according to eq 1:[35]

$$\Delta G^{\ddagger}\ (\text{kcal/mol}) = 4.575 \times 10^{-3} T_{coal}\,[9.972 + \log(T_{coal}/\Delta\nu)] \quad (1)$$

Based on the data for T_{18}-6H, $\Delta G^{\ddagger}$ at 320 K for this interconversion is *ca.* 15 kcal/mol.

It is striking that the only DNA and drug protons exhibiting resonance doubling, *i.e.*, those of DNA residues A_3 and T_4 on the TCCT strand, A_{17} and T_{18} on the AGGA strand, and the calicheamicin aglycone, are spatially proximate in the structural model of the complex (Figure 6b). No resonances of the other DNA residues or of the drug residues A, B, C, D, or E exhibit doubling at low temperature. In fact, the direct contacts of the aglycone with the DNA duplex are precisely at the A_3/T_{18} and T_4/A_{17} base pairs. These observations indicate that the structural difference between the two species is confined to this part of the complex. The cumulative results, including the magnitude of the chemical shift differences observed between the major and minor species, strongly suggest that this exchange phenomenon corresponds to binding of the aglycone to the DNA in two different modes.

A Model for the Double-Strand DNA Cleavage by Calicheamicin. Once activated to form the benzenoid diradical, calicheamicin abstracts hydrogen atoms from both strands of the DNA fragment (Figure 3, Scheme 1). These two hydrogens, *i.e.*, 5′H of the first cytosine from the 5′-end of the TCCT strand (C_5 in our duplex) and 4′H of the nucleotide three base pairs away in the 3′-direction on the AGGA strand (G_{19}), appear to be quite far apart. Using our structural model, the average distance between these hydrogens and each of the two carbons with an unpaired electron can be estimated by subtracting 2.8 Å (the distance between the two carbons in the benzenoid diradical) from 8.2 Å (the distance between C_5-5′H and G_{19}-4′H observed in our models) and dividing by 2. The distance obtained in this way [(8.2 Å–2.8 Å)/2 = 2.7 Å] is too long to allow the formation of the two C–H bonds simultaneously. We conclude that it is highly unlikely that both hydrogen abstractions can occur with the aglycone in a fixed position midway between the two sites (Figure 10).

To explain the DNA cleavage properties of calicheamicin, it is necessary to invoke some dynamic process to alternately reposition the aglycone for abstraction of the hydrogen atoms. Based on our structural model and the detection of two low-energy conformations in the NMR spectra, we propose that this dynamic process involves a slight movement of the aglycone in the minor groove, which is sufficient to allow the carbon radicals of the benzenoid ring to reach the required positions for the formation of the two C–H bonds. The two conformations would then correspond to alternate binding modes for the aglycone, one closer to the C_5 abstraction site on the TCCT strand and the other closer to the G_{19} abstraction site on the AGGA strand. Implicit in this model is the assumption that there are no substantial changes in the structure of the DNA complex when the benzenoid diradical is formed through the Bergman rearrangement, *i.e.*, no major conformational changes occur upon activation of the drug (Scheme 1). Experimental evidence to support this model could conceivably come from a detailed structural characterization of the minor conformer of the calicheamicin–DNA complex, but our efforts to date have been stymied by the small equilibrium population of the minor species in the solution and the problems with cross peak overlap already quite prevalent for the major conformer. The structural model presented here has been generated for the major binding mode but can be readily rearranged without perturbing other parts of the drug or DNA, so that the calicheamicin aglycone is closer to C_5-5′H.

(35) Sandström, J. *Dynamic NMR Spectroscopy*; Academic Press: New York, 1982.

Conclusion

Two complexes, one between d(GCATCCTAGC)·d(GCTAGGATGC) and calicheamicin θ_1^I (**1**) and the other with the calicheamicin oligosaccharide domain (**3**), have been prepared and analyzed by NMR spectroscopy. The striking similarities of the NMR data observed for the two complexes suggest that the oligosaccharide domain of calicheamicin is the primary structural element governing binding and sequence-specific recognition in the DNA minor groove. The observation in the DNA–calicheamicin θ_1^I complex of two species in equilibrium may explain the abstraction of the two distant hydrogens atoms by the benzenoid diradical implicated in the DNA cleavage activity of calicheamicin. According to this hypothesis, the two species identified in the NMR spectra correspond to two distinct binding modes for the aglycone within the DNA minor groove, which allow each radical on the benzenoid system to reach and abstract its intended target. Further insights into the binding and mechanism of action of the calicheamicins may be gained from higher resolution structures of this drug–DNA complex and comparative analysis of complexes formed with other high-affinity binding sites.

Acknowledgment. We thank Prof. D. Kahne for kindly providing us with his manuscript on the analysis of hydroxylamine glycosidic linkages prior to publication. We thank Prof. Dave Case for helpful discussions and Dr. Dee H. Huang for assistance with NMR experiments. L.G.P. is a visiting Assistant Professor from the University of Naples, Italy. Financial assistance was provided by grants from the National Institutes of Health (to K.C.N.) and the American Cancer Society (CH-529 to W.J.C.) and by The Scripps Research Institute.